ISBN: 978-3-95450-184-7 doi:10.18429/JACoW-IPAC2018-THPAK008

SPACE CHARGE AND MICROBUNCHING STUDIES FOR THE INJECTION ARC OF MESA

A.Khan*, O. Boine-Frankenheim
Institut Theorie Elektromagnetischer Felder TU Darmstadt, Germany
C. Stoll
Johannes Gutenberg University Mainz (IKP) Fachbereich Physik Institut für Kernphysik, Germany

Abstract

For intense electron bunches traversing through bends, as for example the recirculation arcs of an energy recovery linac (ERL), space charge (SC) may result in beam phase-space degradation. SC modifies the electron transverse dynamics in dispersive regions along the beam line and causes emittance growth for mismatched beams or for specific phase advances. On the other hand, longitudinal space charge together with dispersion can lead to the microbunching instability (MBI). The present study focuses on the 180° low energy (5 MeV) injection arc lattice for the multi-turn Mainz Energy-recovering Superconducting Accelerator (MESA), which should deliver a CW beam at 105 MeV for physics experiments with an internal target. We will discuss matching conditions with space charge together with the estimated microbunching gain for the arc. The implication for the ERL operation is outlined, using 3D envelope and tracking simulations.

INTRODUCTION

Space charge and microbunching instability are important for low energy, multi-turn ERL machines like MESA [1], which should deliver a high beam quality for precise nuclear and particle physics experiments [2]. Transverse space charge might affect the beam transport matrix and longitudinal space charge (LSC) together with dispersion can lead to the amplification of the initial shot noise by density modulation along the beamline, which is known as MBI [3]. It is important to develop an effective methodology to optimize MESA lattice design against SC by increasing local momentum spread as experiments demand high quality beam with low emittance.

A layout of MESA lattice is shown in Fig. 1. MESA has a 100 keV polarized photo-cathode electron gun with a normal conducting injector linac, which provides very short electron bunches 4.275 ps of energy 5 MeV [1,2]. There are two superconducting linac modules with an energy gain of 25 MeV for each pass, four spreader sections for separating and recombining the beam and two chicanes for injection and extraction of the 5 MeV beam. For beam recirculation there are five arcs to support the beam corresponding to five different energy levels: 55 MeV, 80 MeV, 105 MeV, 130 MeV and 155 MeV.

MESA experimental setups require a flexible low energy injection arc for external beam and energy recovery mode. MESA injection arc is a 5 MeV, 180°, first-order achromat with flexible 1^{st} order momentum compaction R_{56} required for the different isochronous/non-isochronous recirculation modes [4]. Here, R_{56} is the correlation element of individual particle path length s and relative energy deviation δ in linear approximation given as $s = s_0 + R_{56}\delta$, which quantifies the change in path length with energy in the presence of dispersion and computed from 6×6 transport matrix of magnetic elements [5].

ENVELOPE SOLVER WITH 3D SPACE CHARGE

The beam envelopes and lattice functions are obtained by solving the envelope equations by a matrix method, including the linear space charge defocusing such that beam matrix B_s along the longitudinal position s is given by, $B_s = RB_{s_0}R^T$ with R as transport matrix $R(s_0, s_0 + \Delta s) = R_{\Delta s/2}R^{sc}_{\Delta s}R_{\Delta s/2}$. Here, B represents the 6×6 matrix, with elements B_{ij} defined by $B_{ij} = \langle v_i v_j\rangle - \langle v_i\rangle\langle v_j\rangle$, where the averages are taken over the phase space variables and the subscripts i, j runs from 1 to 6 representing x, x', y, y', z, z' [6,7]; R^{sc} is the space charge kick.

For a detailed understanding of the beam dynamics the transverse envelope equations should be coupled with the longitudinal equation. The space charge modified transverse and longitudinal coupled rms envelope equations for the rms beam radii $\sigma_x = \sqrt{B_{11}}$ and $\sigma_y = \sqrt{B_{33}}$ including dispersion [8,9] and longitudinal half bunch length z_m [10] are:

$$\begin{aligned}
&\frac{d^2 z_m}{ds^2} + \left(\kappa_{z_0} - \frac{K_L}{z_m^3}\right) z_m - \frac{\epsilon_z^2}{z_m^3} = 0 \\
&\frac{d^2\sigma_x}{ds^2} + \left(\kappa_x(s) - \frac{K_{sc}}{2X(X+Y)}\right)\sigma_x - \frac{\epsilon_x^2}{\sigma_x^3} = 0 \\
&\frac{d^2\sigma_y}{ds^2} + \left(\kappa_y(s) - \frac{K_{sc}}{2Y(X+Y)}\right)\sigma_y - \frac{\epsilon_y^2}{\sigma_y^3} = 0 \\
&\frac{d^2 D_x}{ds^2} + \left(\kappa_x(s) - \frac{K_{sc}}{2X(X+\sigma_y)}\right) D_x = \frac{1}{R}
\end{aligned} \tag{1}$$

with the coupled relations

$$X = \sqrt{\sigma_x^2 + {D_x}^2\sigma_\delta^2}, Y = \sigma_y \tag{2}$$

and

$$\sigma_\delta = \sqrt{\left(\frac{\sigma'_z}{\eta}\right)^2 + \left(\frac{\epsilon_z}{\eta\sigma_z}\right)^2} \tag{3}$$

* khan@temf.tu-darmstadt.de

ISBN: 978-3-95450-184-7 doi:10.18429/JACoW-IPAC2018-THPAK008

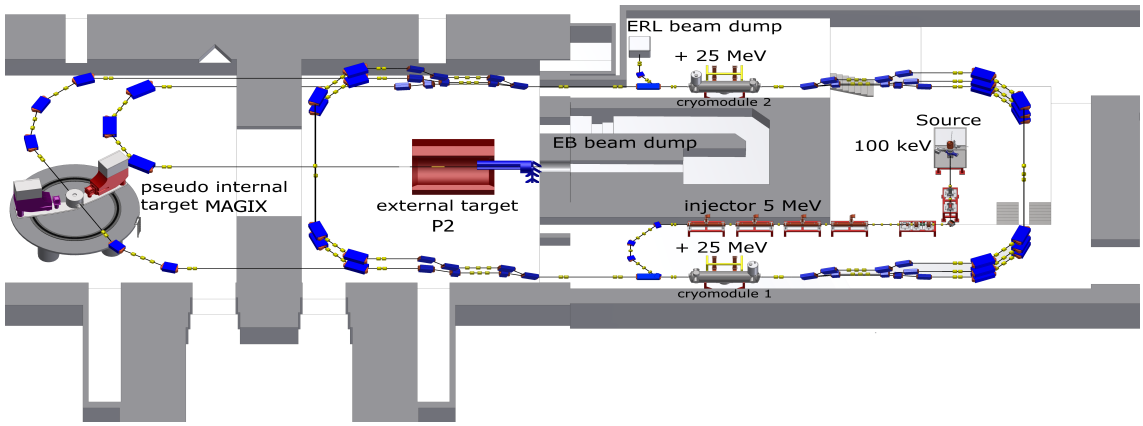

Figure 1: MESA layout.

Here, $\kappa_{x,y}$ and κ_z are the linearized external focusing gradients in transverse and longitudinal plane, respectively; X and Y are effective transverse rms beam radius including dispersion; σ_δ the rms momentum spread; $\epsilon_{x,y}$ the generalized transverse rms emittance [8] and ϵ_z the longitudinal rms emittance defined in terms of rms spread in longitudinal position and rms fractional momentum deviation [10]; $K_L = 3gNr_e/(2\beta^2\gamma^5)$ the longitudinal perveance with geometry factor $g = 0.5 + 2ln(r_p/r_b)$ (r_p and r_b are the the radii of the beam pipe and beam, respectively); N is the number of particles in the bunch; r_e the classical electron radius; η is the phase shift factor; $I = (3qN\beta c)/4z_m$ is the beam peak current; $K_{sc} = eI/\left(2\pi\epsilon_0 m_e(\beta\gamma)^3\right)$ the transverse space charge perveance; $\gamma = E_k/m_e c^2$ and $\beta = \sqrt{1-1/\gamma^2}$ are the relativistic factors; E_k and m_e are the kinetic energy and mass of electron respectively.

The process to find the solutions is as follows: Firstly, the half bunch length z_m is calculated by longitudinal envelope equation, from which one can obtain the beam current and momentum spread. Secondly, based on beam current, K_{sc} is calculated which gives the beam radii and R_{56}, which is an important parameter for LSC induced microbunching instability gain calculations.

LONGITUDINAL SPACE CHARGE INDUCED MICROBUNCHING

MBI is a pervasive occurrence in dispersive beamlines, which potentially affects the beam performance and operation. In its common explanation the instability is driven by longitudinal component of the beam self-fields originating from space charge and coherent synchrotron radiation (CSR). Perturbations in the beam density like shot noise can seed self-fields on micro scale, which then modify energy profile along the bunch.As the beam travels through dispersive beamlines the modified energy profile causes differential longitudinal slippage and induces ripples in the current profile by further amplifying self-fields. The net result of this amplifying loop degrades the beam quality [3, 11].

A physical quantity used to measure the direct consequences of MBI is the microbunching gain, defined as the ratio of initial and final amplitude of density modulations. Analytically, the microbunching gain (ultra-relativistic approx) due to LSC over a distance L_s can be depicted as follows [3]:

$$G \simeq 4\pi \frac{I_0}{I_A} L_s \frac{|Z(k)|}{Z_0} |R_{56}| k e^{-(kR_{56}\sigma_\delta)^2/2} \quad (4)$$

where $Z(k)$ is the longitudinal space charge impedance at modulation wavelength k; Z_0 the vacuum impedance; I_0 the bunch peak current and I_A the Alfven's current.

We adopt the LSC impedance derived in Ref. [12] using a beam model with average uniform average transverse density and circular cross section of radius r_b, it is valid in shorter wavelength limit $\xi_b \gg 1$ and longer wavelength limit when $\xi_b \ll 1$:

$$Z(k) = \frac{i Z_0}{\pi\gamma r_b} \frac{(1 - \xi_b K_1(\xi_b))}{\xi_b} \quad (5)$$

where $\xi_b = kr_b/\gamma$, $r_b \approx 1.7(\sigma_x + \sigma_y)/2$ is beam radius computed from beam envelopes along the beamline.

The analytical results are benchmarked against the particle tracking simulations in ELEGANT [11].

SIMULATION RESULTS

The injection arc of MESA is suppose to be a dual purpose 5 MeV arc with finite momentum compaction R_{56} for energy recovery and external beam mode. A nominal design of arc should deliver fixed beam parameters with zero dispersion after first cryomodule for energy recovery operation.

Our estimation of SC effects are for a typical set of beam parameters listed in Table 1. The simulation of 3D SC for given initial twiss parameters show the increase of the transverse beam envelope along x in Fig. 2 (a), an increase in longitudinal bunch length Fig. 2 (b), non-zero dispersion Fig.2 (c) at the end of the arc and an increase in momentum compaction after second dipole of first achromat Fig. 2 (d) with SC. Therefore, we need an additional knob for arc flexibility against SC defocusing, as matching of arc to get fixed beam parameters after first cryomodule demands a fixed set of twiss parameters at the entrance of module.

ISBN: 978-3-95450-184-7 doi:10.18429/JACoW-IPAC2018-THPAK008

Table 1: Beam Parameters for the Injection Arc of MESA

Parameters [unit]	Symbol	Value
Kinetic energy [MeV]	E_k	5
Current [mA]	I_b	1
Initial beta(x) function [m]	β_{x0}	1.30
Initial beta(y) function [m]	β_{y0}	0.90
Initial alpha(x) function	α_{x0}	−0.17
Initial alpha(y) function	α_{y0}	−0.57
Initial rms mom. spread [/%]	σ_δ	$1 \cdot 10^{-4}$
Initial half bunch length [m]	z_m	$6.405 \cdot 10^{-4}$
Norm. emittance [π mm-mrad]	$\epsilon_{nx,ny}$	2

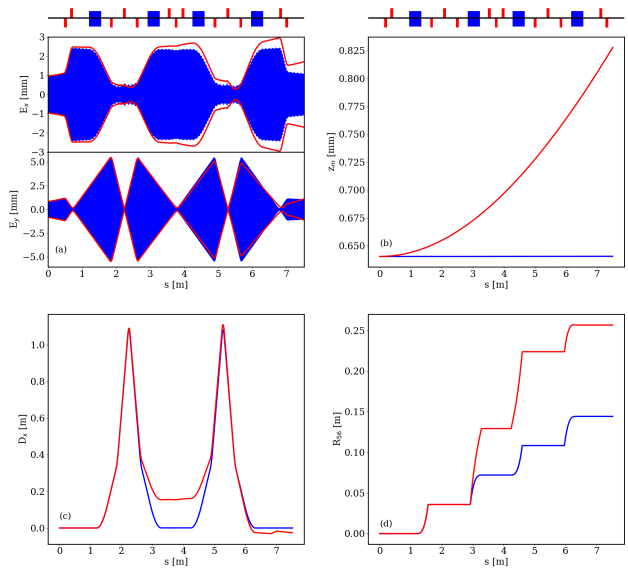

Figure 2: Evolution of beam parameters along the beamline with SC (red) and without SC (blue) (a) Transverse beam envelopes along x and y (b) Longitudinal half-bunch length z_m (c) Dispersion D_x (d) Momentum compaction R_{56} respectively.

In Fig. 3 we compute the MBI gain factor G in density modulations for λ 1 to 100 µm at the end of the arc with and without transverse SC. As expected from the Fig. 2 (d) the gain is amplified with transverse SC. Additionally, there is good agreement of analytical results with the particle tracking simulations in ELEGANT. Figure 4 shows the MBI gain less than 1 at λ 50 µm, 100 µm and 200 µm along the beamline, which predicts there is no microbunching instability due to LSC for the reference beam parameters listed Table 1.

CONCLUSION AND OUTLOOK

The coupled 3D envelope equations including dispersion and LSC microbunching gain is applied to the injection arc of MESA. The analytical results are found to agree with ELEGANT particle tracking simulations. Results show deviation of lattice design parameters of arc with SC. However, there is no microbunching instability in MESA injection arc.

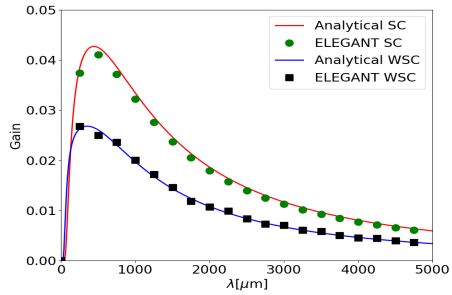

Figure 3: Microbunching gain at the end of the arc as a function of the initial modulation wavelength λ with SC and without SC (WSC). The dots and square are taken from particle tracking simulation by ELEGANT, with total of 20 million macroparticles.

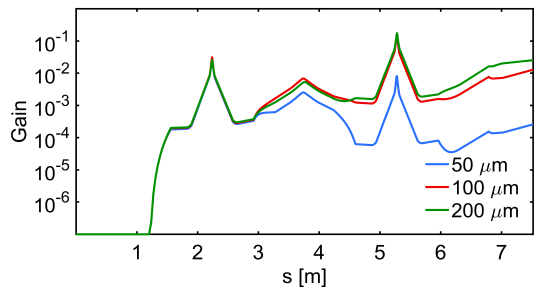

Figure 4: LSC microbunching gain at three different wavelengths (blue) λ = 50 µm, (red) λ = 100 µm and (green) λ = 200 µm along the beamline.

Further studies will include the start to end simulations of MESA lattice with SC.

ACKNOWLEDGEMENT

We are grateful for the financial support provided by DFG through GRK 2128 Accelence project D-3 to study effect of space charge and wake-fields in MESA.

REFERENCES

[1] R. Heine *et al.*, Lattice and start to end simulation of the Mainz Energy Recovering Superconducting Accelerator MESA, *Proceedings of IPAC2014*, MOPRO108 (2014).

[2] K. Aulenbacher*et al.*, Opportunities for parity violating electron scattering experiments at the planned MESA facility, *Hyperfine Interact. 200*, 3 (2011).

[3] E.L Saldin, Longitudinal space charge driven microbunching instability in TTF2 linac, *Nucl. Instr. Meth.*, vol. 483, pp. 516-520 (2002).

[4] F. Hug *et al.*, Injector linac stability requirements for high precision experiments at MESA, *J.Phys: Conf.Ser. 874*, 0122012 (2012).

[5] H. Wiedemann, Particle accelerator physics, *Springer International Publishing Switzerland 2015*, Ch.7-13.

[6] D. Chernin, Evolution of rms beam envelopes in transport system with linear , *Part. Accel. 24*, pp. 29-44 (1988).

[7] Y. Yuan *et al.*, Modeling of second order space charge driven coherent sum and difference instabilities, *Phy. Rev. Accel. Beams 20*, 104201 (2017).

ISBN: 978-3-95450-184-7 doi:10.18429/JACoW-IPAC2018-THPAK008

[8] M. Venturini *et al.*, rms envelope equations in the presence of space charge and dispersion, *Phys. Rev. E 57*, 4725 (1998).

[9] Y.S. Yuan *et al.*, Dispersion-Induced Beam Instability in Circular Accelerators, *Phys. Rev. Lett. 118*, 154801 (2017).

[10] S.Bernal, A practical introduction to beam physics and particle accelerators, *Morgan and claypool publishers 2016*, Ch.5 Longitudinal beam dynamics and radiation.

[11] M. Borland, elegant: A Flexible SDDS-Compliant Code for Accelerator Simulation, APS Light Source Note LS-287 (2000) and Modeling of microbunching instability, *Phys. Rev. ST Accel. Beams 11*, 030701 (2008).

[12] M. Venturini, Models for longitudinal space charge impedance for microbunching instability, *Phys. Rev. ST Accel. Beams 11*, 034401 (2008).